

Compatibility of a model for the QCD-Pomeron and chiral-symmetry breaking phenomenologies

A. A. Natale ¹ and P. S. Rodrigues da Silva ²

Instituto de Física Teórica, Universidade Estadual Paulista

Rua Pamplona, 145, 01405-900, São Paulo, SP - Brazil

Abstract

The phenomenology of a QCD-Pomeron model based on the exchange of a pair of non-perturbative gluons, *i.e.* gluon fields with a finite correlation length in the vacuum, is studied in comparison with the phenomenology of QCD chiral symmetry breaking, based on non-perturbative solutions of Schwinger-Dyson equations for the quark propagator including these non-perturbative gluon effects. We show that these models are incompatible, and point out some possible origins of this problem.

¹e-mail: natale@axp.ift.unesp.br

²e-mail: fedel@axp.ift.unesp.br

1 Introduction

The interpretation of the Pomeron in the framework of QCD is not fully understood. It is expected to be generated at least by two gluons exchange [1]. However, the exchange of two perturbative gluons cannot reproduce the experimental results on diffractive scattering. In order to circumvent such difficulty, Landshoff and Nachtmann [2](LN) proposed a model where the Pomeron is described by the exchange of two non-perturbative gluons, whose properties are dictated by the expected structure of the QCD vacuum. These non-perturbative gluons should not propagate over long distances, i.e. there is a finite correlation length for the gluon field in the vacuum, which should be determined from first principles, and can be understood in terms of gluon condensates [2]. The LN model describes successfully the experimental results of diffractive phenomena using a quite simple ansatz for the non-perturbative gluon propagator [3, 4]. Recently we improved the model using a QCD motivated non-perturbative gluon propagator, where the correlation length is provided by a dynamically generated gluon mass [5].

The remarkable success of this Pomeron model might provide physical insight in the properties of the gluon propagator in the infrared region. It is, therefore, natural to speculate on the ability of such a model to describe other low-energy QCD phenomena, in particular, dynamical chiral symmetry breaking (DCSB). Within the spirit of the LN model, we study the compatibility of both the Pomeron and DCSB phenomenologies. The quark self-energy is computed through the numerical calculation of the Schwinger-Dyson equation (SDE) for the quark propagator, employing the same non-

perturbative gluon propagators as the ones used in the Pomeron phenomenology. According to the traditional approach to the DCSB [6], these self-energies are used to obtain the experimental values of the quantities that characterize the chiral breaking, such as the quark condensate and the pion decay constant.

It is worth mentioning that the existence of a finite correlation length for the gluon field was already proposed ten years before the LN model in a completely different context [7], and it gained strong support by recent lattice simulation of the gluon propagator [8, 9]. Therefore, a study of its phenomenological implications is quite compelling, although there are few places where this phenomenon can be effectively tested.

Using only QCD motivated gluon propagators, *i.e.* propagators determined from the solutions of Schwinger-Dyson equations or obtained from lattice simulation, which satisfy the LN conditions and are constrained by the diffractive scattering data, we show that they do not lead to satisfactory DCSB parameters. In Section II we discuss some of the non-perturbative propagators found in the literature, and show how they are constrained by the diffractive scattering data according to the LN model. In Section III we use the non-perturbative gluon propagators, with the parameters found in the previous section, to compute the relevant quantities for DCSB. In Section IV we discuss the incompatibility found in the previous section and point out the possible origins of such a failure.

2 Diffractive scattering and gluon propagators

There are several experimental features of diffractive scattering that can be computed through the two-gluon exchange model of the Pomeron according to the LN prescription, and here we will choose two simple quantities which can be related to hadron-hadron total cross sections, and show how they constrain the gluon propagators. The first one will be the quark-Pomeron coupling and the second one, the pion-proton total cross section.

The strength of the Pomeron coupling to quarks (β_0) at leading order is given by [2]

$$\beta_0^2 = \frac{1}{36\pi^2} \int d^2 K \left[g^2(K^2) D(K^2) \right]^2, \quad (1)$$

where $g^2(K^2)/4\pi$ is the running quark-gluon coupling, and the value of $\beta_0^2 = 4 \text{ GeV}^{-2}$ is extracted from the proton-proton cross section. Notice that we will be working with Euclidean momenta ($K^2 = -k^2$).

The amplitude of meson-nucleon scattering is [10]

$$\begin{aligned} A = & \ i \frac{32}{9} s \int d^2 K [\alpha D(K^2)][\alpha D((2\mathbf{Q} - \mathbf{K})^2)] \\ & \times 2[f_M(Q^2) - f_M((\mathbf{Q} - \mathbf{K})^2)] \\ & \times 3 \left[f_N(Q^2) - f_N \left(Q^2 - \frac{3}{2}\mathbf{Q} \cdot \mathbf{K} + \frac{3}{4}K^2 \right) \right], \end{aligned} \quad (2)$$

where s is the square of the center-of-mass energy, to the couplings (α) we associate the same momentum of its multiplying propagator, f_M and f_N are respectively the meson and nucleon form factors. The total cross section is

related to this amplitude by

$$\sigma_T = \frac{\text{Im}A(s, t=0)}{s}, \quad (3)$$

and Eq.(2) is computed with the form factors in the pole approximation

$$f_i(K^2) = \frac{1}{\left(1 + \frac{\langle r_i^2 \rangle}{6} K^2\right)}. \quad (4)$$

We will calculate the pion-proton total cross section. Actually, the two gluon exchange model cannot describe the full cross section growth with energy ($\propto s^{0.0808}$), which appears in a recent fit for the $\pi - p$ total cross section [11]

$$\sigma_T^{\pi p} = 13.63s^{0.0808} + 36.02s^{-0.4525}. \quad (5)$$

The model can only accommodate the value 13.63 in the above expression. We used the following mean squared radii for the proton and pion, respectively [12]: $\langle r_p^2 \rangle = 0.67 \text{ fm}^2$ and $\langle r_\pi^2 \rangle = 0.44 \text{ fm}^2$. Inspection of Eq.(1) and Eq.(2) show that they are quite dependent on the gluon propagator expression at $k^2 \rightarrow 0$ and, therefore, well suited to study its infrared behavior.

We will now consider the propagators that satisfy some of the basic assumptions of the LN model: (a) the propagator has a finite correlation length and (b) it is finite at $k^2 = 0$. We will only deal with QCD motivated propagators, *i. e.* those obtained as solutions of the SDE for the gluon polarization tensor, as well as obtained in a lattice simulation. We start with the propagator determined by Cornwall [7], which has already been used by one of us to describe some diffractive scattering processes [5], and has the following

expression

$$D_c^{-1}(K^2) = [K^2 + m^2(K^2)] b g^2 \ln \left[\frac{K^2 + 4m^2(K^2)}{\Lambda^2} \right], \quad (6)$$

where $m^2(K^2)$ is a momentum-dependent dynamical mass

$$m^2(K^2) = m_g^2 \left[\frac{\ln \left(\frac{K^2 + 4m_g^2}{\Lambda^2} \right)}{\ln \frac{4m_g^2}{\Lambda^2}} \right]^{-12/11}. \quad (7)$$

In the above equation m_g is the effective gluon mass, and $b = (11N - 2n_f)/48\pi^2$ is the leading order coefficient of the β function of the renormalization group equation, with $N = 3$ for QCD, and where n_f is the number of flavors taken to be 3. In Eq.(6), the quark-gluon coupling strength g is such that $g \simeq 1.5 - 2$, which was determined from a fit of Eq(6) to the numerical solution of the SDE for the gluon propagator. For the running coupling constant $g(K^2)$ we assume a functional form which interpolates between a constant and the renormalization group asymptotic behavior

$$\alpha_s(K^2) \equiv \frac{g^2(K^2)}{4\pi} = \frac{12\pi/(33 - 2n_f)}{\ln(\frac{K^2}{\Lambda^2} + \tau)}, \quad (8)$$

where $\tau = \kappa^2/\Lambda^2$, and we chose $\kappa = m_g$. Such freeze-out of the coupling constant in the infrared region is consistent with the Cornwall and Papavassiliou [13] study of the trilinear gluon vertex. A similar form for the coupling constant has also been used in many phenomenological applications (see, for instance, Ref. [14] and references therein).

It has also been pointed out that the dynamical gluon mass may have a faster decrease with the momentum [15], according to the operator product expansion (OPE) determination of the ultraviolet behavior of the gluon

polarization tensor [16]

$$\Pi_{UV}(k^2) \sim \frac{34N\pi}{9(N^2 - 1)} \frac{\langle \alpha_s G^2 \rangle}{k^2}, \quad (9)$$

where $\langle \alpha_s G^2 \rangle$ is the gluon condensate. Therefore, to be consistent with the massive Cornwall propagator and with OPE, we will consider a gluon self-energy that interpolates between the constant infrared behavior of Eq.(7) and the ultraviolet one of Eq.(9) which will be given by

$$m^2(K^2) = \mu^2 \theta(\mu^2 - K^2) + \frac{\mu^4}{K^2} \theta(K^2 - \mu^2), \quad (10)$$

where the scale μ^2 will be limited by Eq.(1) and Eq.(2).

Another infrared finite propagator has been found by Stingl and collaborators as a solution of the SDE for the gluon polarization tensor [17]. Its form agrees with that derived by Zwanziger based on considerations related to the Gribov horizon [18], and is given by

$$D_s(K^2) = \frac{1}{K^2 + \frac{\mu_s^4}{K^2}}, \quad (11)$$

where μ_s is a mass scale not determined in Ref. [17]. The term μ_s^4/K^2 is exactly what is expected by OPE analysis whenever a mass scale for the gluon is introduced, and the full solution found in Ref. [17] did contain a mass term, although its consequences were not pursued. It is also interesting to notice that the Bernard *et al.* lattice result for the gluon propagator [8] can be fitted by Eq.(6) as well as Eq.(11).

Finally, Marenzoni *et al.* [9] also performed a lattice study of the gluon propagator in the Landau gauge, obtaining for its infrared behavior the following fit

$$D_m(K^2) = \frac{1}{m_l^2 + ZK^2(\frac{K^2}{\Lambda^2})^\eta}, \quad (12)$$

where m_l , Z and η are constants determined by the numerical simulation. m_l is of $\mathcal{O}(\Lambda \approx 160 \text{ MeV})$, $Z \approx 0.4$ and $\eta \approx 0.5$ what is slightly different from the previous propagators. The results of Bernard *et al.* also show the behavior $(K^2)^\eta$, but with a smaller value for η . In this case all the propagator parameters are determined, and we simply have to see if they are consistent with diffractive scattering and DCSB. All the above propagators were obtained in Landau gauge, except Cornwall's one, whose massive solution was shown to be gauge invariant.

Performing the calculation of the integrals in Eqs. (1) and (2) for each one of the above propagators, we obtained the curves for β_0^2 displayed in Fig.(1), and the pion-proton total cross section shown in Fig.(2) as functions of the gluon mass. From these figures and the experimental values of β_0 , and the pion-proton total cross section, it was possible to establish an effective gluon mass for each propagator. Our results are shown in Table 1.

It is clear from this table that almost all the gluon mass scales that fit the experimental value of β_0 give reasonable (within 10%) values for the total pion-proton cross section, except in the case of the lattice propagator, Eq.(12), where the comparison with the experimental values yields effective gluon masses differing by 35%. It is evident that not only the mass scale plays a role in this phenomenology, but also the functional form of the propagator introduces differences in the calculation, and this is why this problem becomes more interesting, because we can speculate about the infrared behavior of the gluon propagator. As we shall see in the next section, we will fail to obtain DCSB with the above propagators for the gluon mass scales presented in Table 1.

3 DCSB with LN type propagators

We discuss dynamical chiral symmetry breaking following the traditional approach [6]. This consists in solving the Schwinger-Dyson equation (SDE) for the quark propagator and look for a mass term dynamically generated in this propagator.

The Schwinger-Dyson equation for the quark propagator is

$$S^{-1}(p) = \not{p} - i \frac{4}{3} \int \frac{d^4 q}{(2\pi)^4} \gamma_\mu S(q) \Gamma_\nu(p, q) g^2 D^{\mu\nu}(p - q), \quad (13)$$

where we write the gluon propagator in the form

$$g^2 D^{\mu\nu}(q) = \frac{4\pi\alpha(-q^2/\Lambda^2)}{q^2} \left(-g^{\mu\nu} + \frac{q^\mu q^\nu}{q^2} \right). \quad (14)$$

The propagator has been written in the Landau gauge, which will be used throughout our work. In the above equations $\Gamma_\nu(p, q)$ is the vertex function, and $\alpha(-q^2/\Lambda^2)$ is the QCD running coupling constant given by Eq.(8).

To proceed further we also need to introduce an ansatz for the quark-gluon vertex $\Gamma^\mu(p, q)$, which must satisfy a Slavnov-Taylor identity that, when we neglect ghosts, reads

$$(p - q)_\mu \Gamma^\mu(p, q) = S^{-1}(p) - S^{-1}(q). \quad (15)$$

This identity constrains the longitudinal part of the vertex, and if we write $S^{-1}(p)$ in terms of scalar functions

$$S^{-1}(p) = A(p) \not{p} - B(p), \quad (16)$$

we find the solution [19]

$$\begin{aligned} \Gamma^\mu(p, q) &= \frac{(p - q)^\mu}{(p - q)^2} \left([A(p^2) - A(q^2)] \not{q} - [B(p^2) - B(q^2)] \right) \\ &\quad + A(p^2) \gamma^\mu + \text{transverse part}, \end{aligned} \quad (17)$$

which is a much better approximation than the use of the bare vertex [20]. Assuming that the transverse vertex part vanishes in the Landau gauge we obtain

$$D^{\mu\nu}(p-q)\Gamma_\nu(q,p) = D^{\mu\nu}(p-q)A(q^2)\gamma_\nu, \quad (18)$$

and arrive at the approximate Schwinger-Dyson equation

$$[A(p^2) - 1] \not{p} - B(p^2) = i \frac{4}{3} \int \frac{d^4q}{(2\pi)^4} g^2 D^{\mu\nu}(p-q)\gamma_\mu \frac{A(q^2)}{A(q^2) \not{q} - B(q^2)} \gamma_\nu. \quad (19)$$

Going to Euclidean space, we will be working with the following nonlinear coupled integral equations for the quark wave-function renormalization and self-energy

$$\begin{aligned} [A(P^2) - 1]P^2 &= \frac{16\pi}{3} \int \frac{d^4Q}{(2\pi)^4} \frac{\alpha((P-Q)^2/\Lambda^2)}{\Phi[(P-Q)^2]} \\ &\times \left(P.Q + 2 \frac{P.(P-Q)Q.(P-Q)}{(P-Q)^2} \right) \\ &\times \frac{A^2(Q^2)}{A^2(Q^2)Q^2 + B^2(Q^2)}, \end{aligned} \quad (20)$$

$$B(P^2) = 16\pi \int \frac{d^4Q}{(2\pi)^4} \frac{\alpha((P-Q)^2/\Lambda^2)}{\Phi[(P-Q)^2]} \frac{A(Q^2)B(Q^2)}{A^2(Q^2)Q^2 + B^2(Q^2)}, \quad (21)$$

where $Q^2 = -q^2$ and $P^2 = -p^2$, and we introduced a function $\Phi[(P-Q)^2]$ which, in the case of the perturbative propagator, is simply $\Phi[(P-Q)^2] = (P-Q)^2$, for a massive bare gluon it will have the form $\Phi[(P-Q)^2] = (P-Q)^2 + m_g^2$, and will be more complex expression according to the propagators we discussed in the previous section.

The numerical code we used to solve the above equations is the same of Ref. [21], and for each one of the propagators in Section II we substitute: (a) $\Phi(K^2) = D_c^{-1}(K^2)$, (b) $\Phi(K^2) = D_{cm}^{-1}(K^2)$, (c) $\Phi(K^2) = D_s^{-1}(K^2)$ and

(d) $\Phi(K^2) = D_m^{-1}(K^2)$. After obtaining for each case the function $A(p^2)$ and $B(p^2)$, we can compute the quark condensate, which is expressed as

$$\langle\bar{q}q\rangle = -12i \int^\Lambda \frac{d^4p}{(2\pi)^4} \frac{Z(p^2)M(p^2)}{p^2 - M^2(p^2)}, \quad (22)$$

where $Z^{-1}(p^2) = A(p^2)$ and $M(p^2) = B(p^2)/A(p^2)$, and we will also calculate the pion decay constant, which in terms of the functions A and B of Eq.(20) and Eq.(21) is given by

$$\begin{aligned} f_\pi^2 &= -12i \int \frac{d^4p}{(2\pi)^4} \frac{AB}{(A^2p^2 - B^2)^2} [AB \left(1 + \frac{p^2}{2} \frac{d\ln A}{dp^2}\right) \\ &\quad + \frac{p^2}{2} \left(B \frac{dA}{dp^2} - A \frac{dB}{dp^2}\right) \left(1 + p^2 \frac{d\ln A}{dp^2}\right)]. \end{aligned} \quad (23)$$

For all the propagators discussed here, with the respective gluon mass scales given in Table 1, we have not obtained dynamical quark mass generation! Our results for f_π and $\langle\bar{q}q\rangle$ are identically zero (at least ten orders of magnitude below the scale Λ). The gluon mass scales of Table 1 are too large, in the sense that they cause a too strong screening of the force necessary to generate the symmetry breaking. To illustrate this incompatibility we present in Fig.(3) the curve of the dynamically generated quark mass ($M(p^2 = 0)$) against the gluon mass, in the case of the Cornwall propagator (Eq.(6)), which gives the largest signal of mass generation that we obtained among all the propagators described above. Notice that in Fig.(3) to obtain dynamical quark masses of $\mathcal{O}(300 \text{ MeV})$, we would need a gluon mass almost half the value necessary to satisfy the constraints from diffractive scattering.

The inconsistency between diffractive scattering and the chiral symmetry breaking phenomenologies is not only a matter of adjustment of the infrared

gluon mass scale, this scale really plays a different role in both cases. We need large gluon masses ($m_g \gg \Lambda$) to soften the t-channel singularity in diffractive scattering, but smaller gluon masses if we do not want to erase the dynamical quark mass generation. It is obvious that we have an inconsistency, although it is far from clear which is the solution. Nevertheless, this comparison of phenomenologies gives a powerful tool to constrain the detailed behavior of the infrared gluon propagator.

4 Conclusions

The LN Pomeron model is able to explain a large amount of experimental data on diffractive scattering [4, 5], making use of an infrared finite gluon propagator. As we have seen in Section 2, we need only a unique gluon mass scale to fit the pomeron-quark coupling and the pion-proton total cross section. On the other hand we have an extensive and successful phenomenology of DCSB, which was performed mostly with a “perturbative” ($1/k^2$) gluon propagator. In Section 3 we followed the standard procedures to compute the dynamical quark mass, quark condensate and pion decay constant, with the same non-perturbative propagators prescribed by the LN model. Both phenomenologies are inconsistent. We need large gluon masses for diffractive scattering, and small ones to generate appropriate chiral symmetry breaking parameters!

There is a clear difference between our calculation of DCSB with the previous ones. The use of “massive” propagators clearly screens the force necessary to generate the chiral symmetry breaking, and it is probably in

this direction that we may look for troubles, another possibility would imply that the LN model is incorrect, or that the standard phenomenology of DCSB has nothing to do with a finite correlation length for gluons. Let us discuss about each one of these possibilities. The first common point to both phenomenologies is the existence of a mass scale for the gluon propagator, however, there is another claimed form for the gluon propagator in the infrared region, namely, $1/k^4$ (see [22] and references therein). In view of the theoretical arguments of Ref. [7, 16, 17, 18] about gluon mass scales, and the numerical simulations on the lattice [8, 9], we were compelled to assume that the gluon field definitively has a finite correlation length in the vacuum, discarding the $1/k^4$ solution.

The gluon propagator being infrared finite, there is no comparison with the experimental data which would force us to abandon the LN model, and it remains to see if the DCSB phenomenology with such propagator is still consistent. Another difference to standard DCSB calculations is the use of the QCD running coupling constant given by Eq.(8), which, as we said previously, is consistent with a study of the trilinear gluon vertex, and naturally embodies the freezing of the coupling at the relevant gluon mass scale [13]. Both phenomenologies, diffractive scattering and DCSB, depend strongly on the behavior of this coupling in the infrared, however, its effect works basically in the same direction, i.e. increasing the coupling in the infrared we increase the diffractive scattering parameters as well as the dynamical quark mass. Therefore, there will not be much room to changes in this direction. Finally, if we assume that the LN Pomeron model is correct, the gluon field has a finite correlation length in the vacuum, and the coupling constant has

the freezing-out referred to above, we are forced to say that the dynamical quark mass is not generated by single-gluon forces, and the usual calculation of dynamical quark masses should be modified when the gluon mass is taken into account. Actually, this view is not new, studying the coupled fermion gap and vertex equations for DCSB in QCD it was also found an incompatibility [23], and it was argued that the standard technique of using one-gluon exchange in the SDE is not suitable when we consider the effect of massive gluons, and our work, in a different way, corroborates their result.

We finalize stressing that we are still far from knowing all the subtleties of QCD, and we have formalized the incompatibility between a QCD Pomeron model and DCSB. We believe that the confront of these different phenomenologies may provide strong constraints on the infrared behavior of the gluon propagator.

Acknowledgments

This research was partially supported by the Conselho Nacional de Desenvolvimento Científico e Tecnológico (CNPq)(AAN), and Fundação de Amparo a Pesquisa do Estado de São Paulo (FAPESP)(PSRS). We would like to thank Jean-Rene Cudell and Francis Halzen for their comments on a previous manuscript, and also G. Krein for discussions, and for helping us with the numerical code of Ref.[21]. We are grateful for the kind hospitality at the Institute for Elementary Particle Physics Research, University of Wisconsin - Madison (AAN), and at the International Centre for Theoretical Physics (ICTP) (PSRS), where part of this work was done.

References

- [1] F. E. Low, Phys. Rev. **D12**, (1975) 163; S. Nussinov, Phys. Rev. Lett. **34**, (1975) 1268.
- [2] P. V. Landshoff and O. Nachtmann, Z. Phys. **C35**, (1987) 405.
- [3] A. Donnachie and P. V. Landshoff, Phys. Lett. **B185**, (1987) 403; Nucl. Phys. **B311**, (1988/89) 509.
- [4] J. R. Cudell, Nucl. Phys. **B336**, (1991) 1.
- [5] F. Halzen, G. Krein and A. A. Natale, Phys. Rev. **D47**, (1993) 295; M. B. Gay Ducati, F. Halzen and A. A. Natale, Phys. Rev. **D48**, (1993) 2324.
- [6] C. D. Roberts and A.G. Williams, *Dyson-Schwinger Equations and their Applications to Hadron Physics*, to appear in Progress in Particle and Nuclear Physics, edited by A. Faßler (Pergamon Press, Oxford 1994).
- [7] J. M. Cornwall, Phys. Rev. **D26**, (1982) 1453; in *Deeper Pathways in High-Energy Physics*, edited by B. Kursunoglu, A. Perlmutter and L. Scott (Plenum, New York, 1977), p. 683; Nucl. Phys. **B157**, (1979) 392.
- [8] C. Bernard, C. Parrinello and A. Soni, Phys. Rev. **D49**, (1994) 1585.
- [9] P. Marenzoni et al., preprint hep-ph 9410355; P. Marenzoni, G. Martinelli, N. Stella and M. Testa, Phys. Lett. **B318**, (1993) 511; P. Marenzoni, G. Martinelli, and N. Stella, Nucl. Phys. **B455**, (1995) 339.

- [10] J. F. Gunion and D. E. Soper, Phys. Rev. **D15**, (1977) 2617; E. M. Levin and M. G. Ryskin, Yad. Fiz. **41**, (1985) 1622 [Sov. J. Nucl. Phys. **41**, (1985) 1027]; J. Dolejsi and J. Hufner, Z. Phys. **C54**, (1992) 489.
- [11] A. Donnachie and P. V. Landshoff, Phys. Lett. **B296**, (1992) 227.
- [12] B. Povh and J. Hufner, Phys. Rev. Lett. **58**, (1987) 1612; Phys. Lett. **B245**, (1990) 653.
- [13] J. M. Cornwall and J. Papavassiliou, Phys. Rev. **D40**, (1989) 3474.
- [14] C. D. Roberts and B. H. J. McKellar, Phys. Rev. **D41**, (1990) 672.
- [15] J. M. Cornwall and Wei-Shu Hou, Phys. Rev. **D34**, (1986) 585.
- [16] M. Lavelle, Phys. Rev. **D44**, (1991) R26.
- [17] M. Stingl, Phys. Rev. **D34**, (1986) 3863; U. Habel et al., Z. Phys. **A336**, (1990) 423-433.
- [18] D. Zwanziger, Nucl. Phys. **B378**, (1992) 525.
- [19] G. Krein, P. Tang and A. G. Williams, Phys. Lett. **B215**, (1988) 145.
- [20] D. C. Curtis, M. R. Pennington and D. A. Walsh, Phys. Lett. **B249**, (1990) 528.
- [21] A. G. Williams, G. Krein and C. D. Roberts, Ann. Phys. (NY) **210**, (1991) 464.
- [22] K. Buttner and M. R. Pennington, Phys. Rev. **D52**, (1995) 5220; Phys. Lett. **B356**, (1995) 354.
- [23] J. Papavassiliou and J. M. Cornwall, Phys. Rev. **D44**, (1991) 1285.

Figure Caption

Table 1 Gluon masses (in MeV) obtained fitting β_0 and $\sigma_{\pi p}$ for the several propagators discussed above. We denote by D_{cm} the gluon propagator given by Eq.(6) with the dynamical gluon mass given by Eq.(10).

Fig. 1 Curves for β_0^2 as a function of the gluon mass. We constrain the gluon mass by fixing $\beta_0^2 = 4.0\text{GeV}^{-2}$. Each gluon propagator is represented by: dashed line (D_c), dash-dotted line (D_m), dotted line (D_s), solid line (D_{mc}).

Fig. 2 Curves for pion-proton total cross section as a function of the gluon mass. The constraint on the gluon mass comes from fixing the value $\sigma_{\pi p} = 13.63$ mb. The gluon propagators are represented by: dashed line (D_c), dash-dotted line (D_m), dotted line (D_{mc}), solid line (D_s).

Fig. 3 Dynamically generated quark mass for the Cornwall's gluon propagator as a function of the gluon mass.

Propagator	β_0	$\sigma_{\pi p}$
D_c	760	779
D_{cm}	513	472
D_s	422	387
D_m	525	388

Table 1:

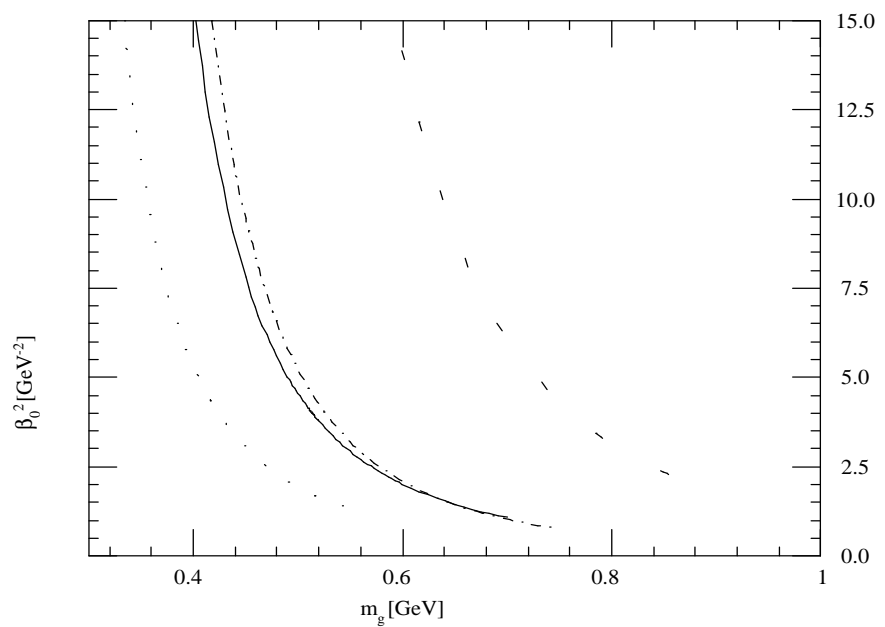


Figure 1:

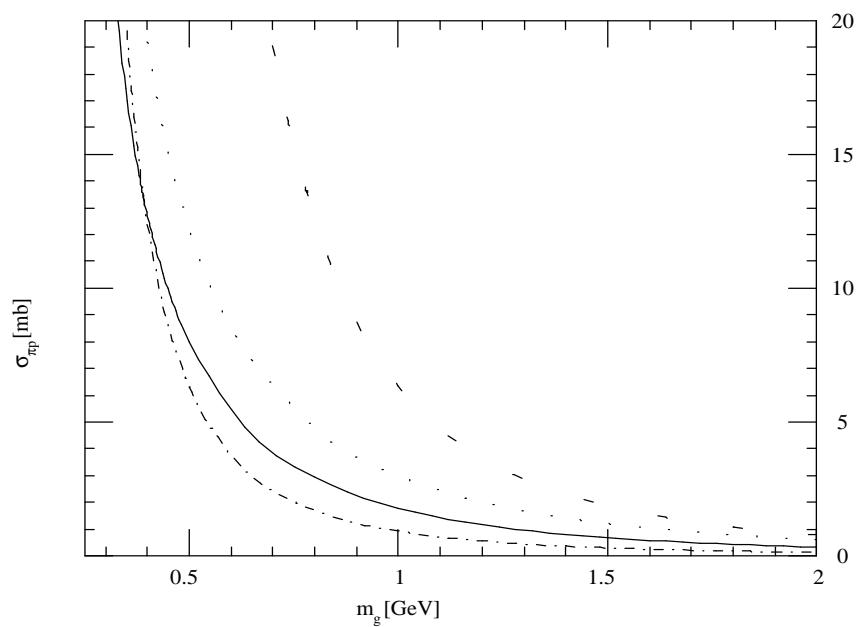


Figure 2:

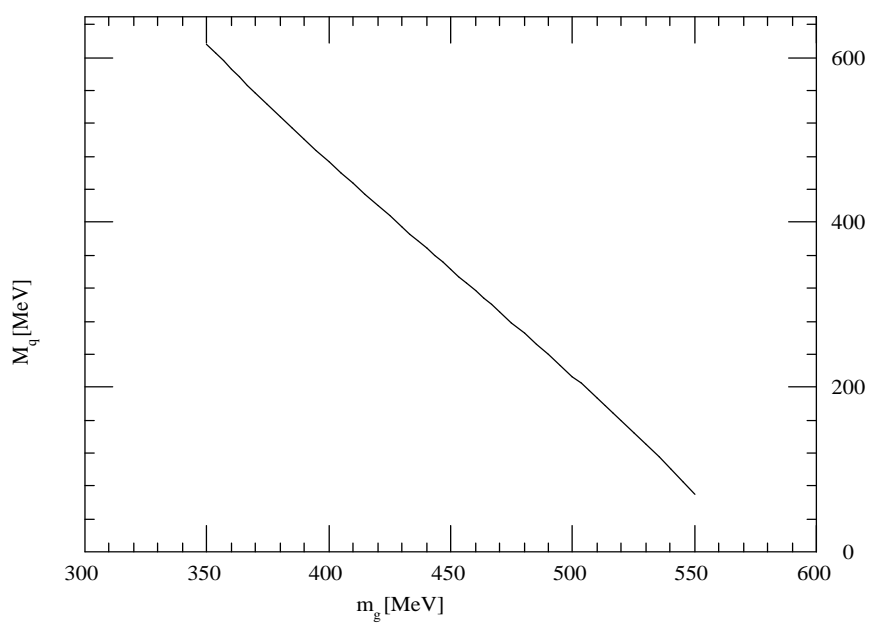


Figure 3: